1998 IEEE INTERNATIONAL FREQUENCY CONTROL SYMPOSIUM

# ACCURATE FREQUENCY COMPARISONS AT THE $1x10^{-15}$ LEVEL

T. E. Parker, D. A. Howe and M. Weiss

National Institute of Standards and Technology
Time and Frequency Division, 847.5
325 Broadway
Boulder, CO 80303 USA

## Abstract

Increased fractional frequency uncertainties in comparing two cesium-fountain primary frequency standards due to a long-baseline comparison process are examined. These include frequency uncertainties introduced by the time-transfer process and uncertainties introduced by possible long-term dead time in the fountain operation. Using common-view GPS it may take up to 40 days to reduce the time-transfer fractional frequency uncertainty to $1x10^{-15}$. A combination of common-view GPS and two-way satellite time and frequency transfer can reduce this to 24 days. With a very low noise local oscillator such as a cavity-tuned hydrogen maser, distributed fountain dead times as large as 87% can be present and yet contribute only an additional uncertainty of less than $3.3x10^{-16}$.

KEY WORDS - time transfer, noise, dead time, cesium-fountain

## Introduction

In the near future there will be two or more operating cesium-fountain primary frequency standards capable of frequency accuracies at or near $1x10^{-15}$. However, these standards will most likely be separated by thousands of kilometers and the task of comparing the standards without degrading their declared uncertainty is formidable. The procedures for determining the basic uncertainty of the fountain standards are not the subject of this paper, but here we will consider only the potential sources of increased uncertainty due to the comparison process.

Figure 1 shows a simplified diagram of the comparison process. The purpose of the comparison is to determine the frequency difference between the two primary standards, P(A) and P(B). To accomplish this three frequency differences are measured. These are: (1) the frequency difference between the local oscillator, LO(A), and the primary standard, P(A), at site A, (2) the frequency difference between LO(A) and LO(B), and (3) the frequency difference between LO(B) and P(B). Fractional frequency uncertainties associated with any of the three measurement processes must be added in quadrature with the basic evaluated uncertainties of the two primary standards.

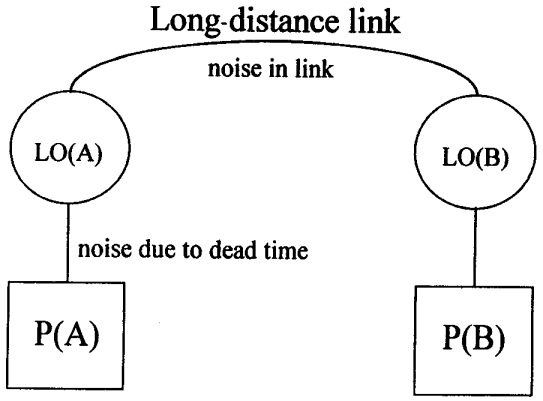


Figure 1 Illustration of frequency comparison process.

The local oscillators at sites A and B are linked by a long-distance time-transfer system that compares the phase (or time) difference of the two LO's over a test interval. The noise in the time-transfer link results in an uncertainty in knowing the phase difference and hence the frequency difference of the two LO's. This frequency uncertainty is a function of the uncertainty in the time (phase) difference and the length of the interval over which the time difference is measured. In comparing two clocks it is essential to know the time difference only at the beginning and end of the test interval. Therefore, the time-transfer measurement does not need to be

continuous. However, it may be helpful to make a number of time difference measurements clustered around the beginning and end points to average down white phase noise.

The standard C/A-code common-view GPS time-transfer technique generally has a $\sigma_x(\tau)$ instability of approximately 1 ns at time intervals of one day or longer. This corresponds to fractional frequency variations of the transfer medium on the order of $10^{-14}$ at two days and $10^{-15}$ at twenty days. Traditional analysis techniques such as $\sigma_x(\tau)$, Mod $\sigma_y(\tau)$, or $\sigma_y(\tau)$ are based on the second difference of a time series, which is of course necessary when dealing with clock frequency offsets and clock noise. However, the frequency *uncertainty* introduced by a time-transfer process is determined by a first difference of the time series that represents the time-transfer noise. The standard variances can serve as a measure of time-transfer frequency uncertainty only if clearly defined relationships exist between the first and second differences of a time series. Such relationships exist only if all instabilities are caused by well-defined, stationary, noise processes. Also sufficient time must be available to fully characterize the slow noise processes. In complex systems these requirements may not always be met.

One can eliminate clock frequency offset and clock noise and still keep the time-transfer instabilities by taking the difference of two clock comparison data sets obtained with different (and independent) time-transfer techniques. This makes possible an analysis based on the first difference of a time series. We will present here a technique for calculating directly the contribution to frequency uncertainty caused by instabilities in a time-transfer system.

It will be shown that comparison times approaching 40 days may be required to obtain a fractional frequency uncertainty of $10^{-15}$ if only one time-transfer technique such as common-view GPS is used. This is an uncomfortably long time, which is vulnerable to one-time random events such as equipment failures, etc. Improved time-transfer techniques are clearly needed. Fortunately several possibilities are on the horizon, but they are not yet fully developed and it is very likely that some of the first comparisons may be made with common-view GPS and/or two-way satellite time and frequency transfer (TWSTFT). Information from primary frequency standards is also used in the generation of International Atomic Time (TAI), which does not approach the $1 \times 10^{-15}$ level until approximately 40 or 50 days. Thus an optimum comparison to TAI also requires long evaluation times. This raises the issue of operating a cesium-fountain standard continuously for many tens of days. Since such operation is likely to be a problem, we must also consider the impact of fountain dead time on the uncertainty of the frequency comparison.

The primary standards at sites A and B are basically very high-quality frequency discriminators, so they measure frequency rather than time (or phase). The frequency stability of the LO's is not relevant if the primary standards operate continuously, since the LO frequencies will drop out of the comparison. However, if the primary standards do not operate continuously the situation is very different. We are not considering here the toss-to-toss dead time of order 1 second which may degrade the short-term stability of the fountain due to LO noise. Here we are concerned with dead times on the order of many days out of an interval of tens of days. In this case long-term frequency information is lost and the average frequency of the LO is known with less precision. This introduces an additional uncertainty in knowing the frequency difference between the primary standard and the local oscillator, which depends on the noise characteristics of the local oscillator. Methods are presented here for estimating the fractional frequency uncertainty due to long-term distributed fountain dead time.

## Time-transfer Instabilities

In this paper we are primarily interested in frequency comparisons, so accurate knowledge of time-transfer delays is not important here. Our main interest is in quantifying the variations in these delays. However, precisely knowing the characteristics of the instabilities in a time-transfer system is a very difficult task, particularly when you are trying to evaluate state-of-the-art techniques. One could in principle quantify the noise of a time-transfer process by comparing it to a much more stable technique. But then we would want to use the more stable technique instead.

However, there are a number of ways to gain some information on the nature and level of time-transfer instabilities in state-of-the-art systems. One traditional method is to calculate the time deviation, $\sigma_x(\tau)$, of two high-stability clocks compared via the time-transfer technique of interest. A $\sigma_x(\tau)$ analysis is very useful in identifying noise types. Figure 2 shows $\sigma_x(\tau)$ for UTC(USNO)-UTC(NIST) as determined via common-view GPS over a 200 day interval. The curve is calculated using individual tracks and is shown without measured ionospheric or precise orbit corrections. For comparison an internal measurement of UTC(NIST) is also shown. Internal data for UTC(USNO) is not presented since it is comparable to or quieter than UTC(NIST). Both curves in Fig. 2 show evidence of white phase noise below $\tau$ = 1 day, but the common-view noise is much larger. (The

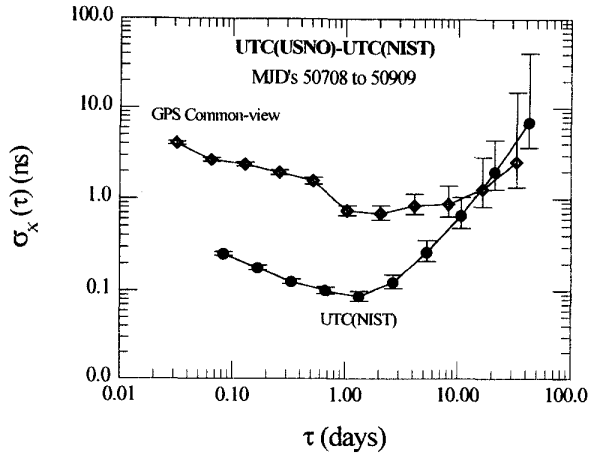


Figure 2 Noise analysis of a GPS common-view comparison of UTC(NIST) with UTC (USNO).

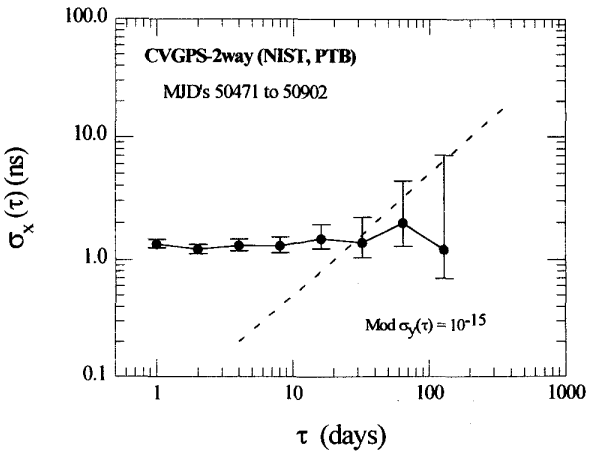


Figure 4 Time deviation of the data in Fig. 3.

white phase noise evident in the internal measurement of UTC(NIST) is from the microstepper used to steer UTC(NIST).) The spacing of the GPS data is not strictly periodic, but this has a negligible effect on the calculation of $\sigma_X(\tau)$ [1]. Also, the spacing for the internal measurement of UTC(NIST), though periodic, is not the same as that of the GPS data. Since white phase noise levels are sensitive to the details of the data-collection procedures and the measurement hardware, a comparison of the two curves must be done with caution. However, the internally measured noise level in Fig. 2 would be even lower if its data had been averaged in the same fashion as the GPS data. Thus the upper curve is reasonably free of clock noise out to about 10 days. The characteristics of the transfer noise are that it is white

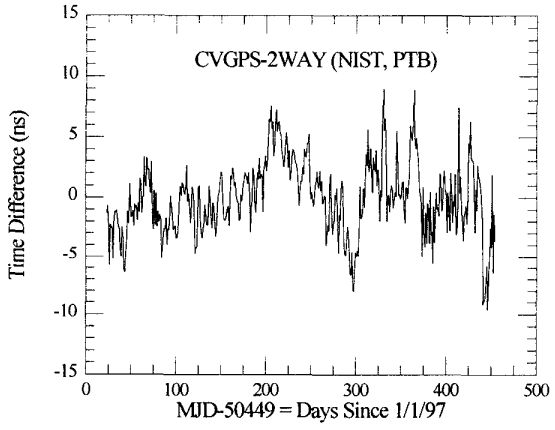


Figure 3 Difference of GPS common-view and TWSTFT for the NIST/PTB link.

phase out to about 1 day, but with a hint of a diurnal effect (weak peak at $\tau \approx 1/2$ day). From one day to about ten days it is flicker phase in nature. The minimum noise level is about 800 ps at 2 days.

Another approach to analyzing time-transfer noise is to compare two independent time-transfer methods for the same two clocks. Figure 3 is a time series showing the difference of common-view GPS (one day averages) and TWSTFT between clocks at the National Institute of Standards and Technology (NIST) and the Physikalisch-Technische Bundesanstalt (PTB). The data cover an interval of 431 days in 1997 and 1998. Since two-way measurements are made only every second or third day, the TWSTFT data had to be interpolated to match the GPS data. By taking the difference of the two data sets the clock noise and offset are removed. Figure 4 is a plot of $\sigma_X(\tau)$ for this data. Note that the noise is flicker phase out to about 100 days, indicating that long-term clock noise is not present. This is a major advantage of the approach since we are primarily interested in the long-term stability characteristics of the transfer process.

Unfortunately, this approach gives the combined noise of the two time-transfer techniques. Comparing the NIST and PTB clocks by individual transfer techniques as in Fig. 2 indicates that the noise levels of common-view GPS and TWSTFT are both on the order of 1 ns at a few days for the NIST/PTB links, but we have no way of knowing the relative noise levels of the two techniques in the long-term (beyond about 10 days). Most likely the noise level in Fig. 4 is too high for GPS noise alone (it should be reduced by $1/\sqrt{2}$ if the two techniques have equal noise levels), but there may be common-mode fluctuations in the two techniques. Without knowing the details of possible common-mode fluctuations it is

impossible to tell whether the combined noise is larger or smaller than that of the individual techniques.

A second approach that removes clock noise is to make closure measurements among three remote locations. Unfortunately this gives the sum of three time transfers and also does not reveal any environmental sensitivities in the ground equipment. Thus this technique also has its weaknesses. To fully characterize the noise of a state-of-the-art time-transfer technique one needs three truly independent techniques of comparable stability so that a three-corner-hat analysis can be performed. Unfortunately these do not exist. Consequently, we are left with the situation of not knowing precisely what the levels of instabilities are in either common-view GPS or TWSTFT. The best we can do is make an estimate. Therefore, we will use the data of Fig. 3 as an estimate of GPS common-view (or TWSTFT) noise for the NIST/PTB link and accept that it may be pessimistic by something on the order a factor of $\sqrt{2}$. Nevertheless, it is useful as an example to illustrate how the frequency uncertainty of a time-transfer technique is calculated. Some advantage can be gained by averaging the LO frequency differences obtained with two time-transfer techniques and this will be discussed later.

The dashed line in Fig. 4 indicates a frequency stability of $1\times10^{-15}$ in Mod $\sigma_y(\tau)$. The intersection of this line with the solid line indicates that it will take something on the order of 30 days to reach a frequency stability of $1\times10^{-15}$. However, as mentioned earlier, Mod $\sigma_y(\tau)$, and $\sigma_y(\tau)$ may not be a good measure of frequency uncertainty in a time-transfer link under some circumstances. Since they are derived from the second difference of a time series they may not properly quantify the frequency uncertainty of some slow processes. A time-transfer system is by definition not a frequency generator, so we must not exclude slow processes that constitute a real frequency error. A more direct way to estimate the frequency error introduced by the time-transfer process is to perform a first difference on the time series as illustrated in Fig. 5. No assumptions have to be made regarding the relationships between first and second differences, and furthermore only half the time is needed to quantify the instabilities. The data shown in Fig. 5 is a subset of the data in Fig. 3.

In Fig. 5 let us define a test interval T, that will generally be chosen to be long enough to give the desired frequency uncertainty, but its length will also be influenced by external factors such as how long your equipment will run, or how much patience you have. Also we will define an interval A over which the time difference values $x_t$ will be averaged to give $\bar{x}_t$. The interval A can be much smaller than T/2. By taking the difference between $\bar{x}_{t+\tau}$ at the end of the interval and $\bar{x}_t$ at

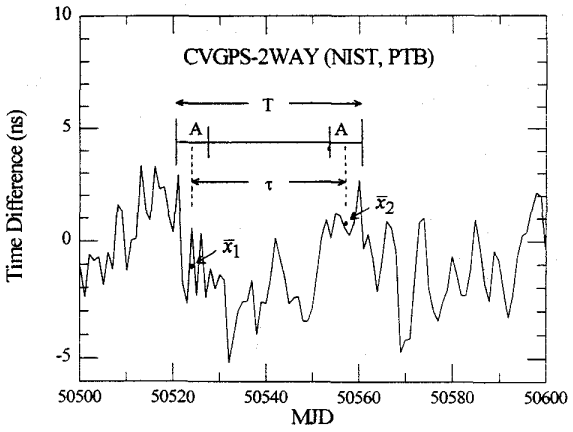


Figure 5 Parameters used for the first difference.

the beginning, and dividing by $\tau$ = T-A one gets the fractional frequency error caused by the instabilities in the time-transfer process. This is similar (but not identical) to how frequency is defined in Mod $\sigma_y(\tau)$. From this a statistical frequency uncertainty, $\sigma_{tt}(T,\tau)$, can be defined as shown below.

$$\sigma_{tt}^2(T,\tau) = \frac{\left\langle (\bar{x}_{t+\tau} - \bar{x}_t)^2 \right\rangle}{\tau^2} \qquad (1)$$

This is just the mean square fractional frequency of the time-transfer data set. If the time-transfer process has no instabilities (slow or fast) then $\sigma_{tt}(T,\tau)$ will be equal to zero.

One could also use linear regression to obtain a measure of the slope (frequency) of the time series, which would be optimum for white phase noise. For random-walk phase (white frequency) the use of endpoints (with A << T), as in Eq. 1, is optimum. However, we are dealing here with flicker phase noise so the situation is not clear. More importantly, when comparing two clocks, the cumulative time error uses the time end points only. Therefore, it is felt that quantifying the frequency uncertainty of the transfer process should be consistent with the procedures used in a clock comparison process, that is, using the end points.

Figure 6 shows $\sigma_{tt}(T,\tau)$ as calculated from the data in Fig. 3. The four solid lines represent values calculated for T = 10, 20, 30 and 40 days, with A ranging from 1 to 10 days. As one would expect $\sigma_{tt}(T,\tau)$ decreases approximately as 1/T. However, increasing A, while holding T constant, has little effect. No matter what value of A is used, it takes about 40 days to reach a level of

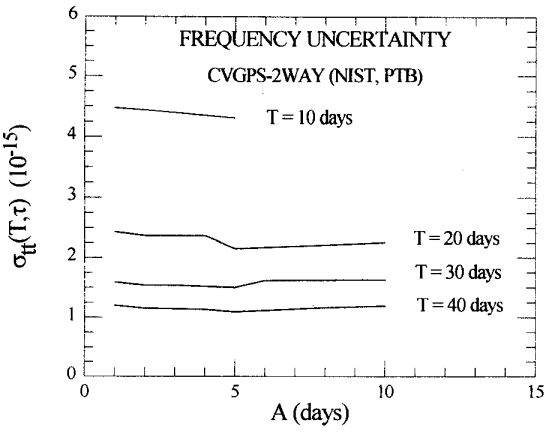


Figure 6 Frequency uncertainty due to time-transfer noise.

frequency uncertainty close to $1x10^{-15}$. Confidence limits are not shown since they have not been calculated for $\sigma_{tt}(T,\tau)$ yet.

The weak dependence on A can be explained by noting that the reduced uncertainty in $\bar{x}_t$ obtained by averaging is counteracted by the decrease in $\tau$ that results from a larger A. If the transfer noise were white phase a stronger dependence on A would be observed. However, as seen in Fig. 2, a one-day average removes virtually all the white phase noise.

Figure 7 shows the distribution of the individual first difference measurements that go into calculating $\sigma_{tt}(T,\tau)$ for T = 40 days and A = 1. Just slightly less than 62 percent of the values fall within +/- $1x10^{-15}$, indicating that the distribution function is close to gaussian.

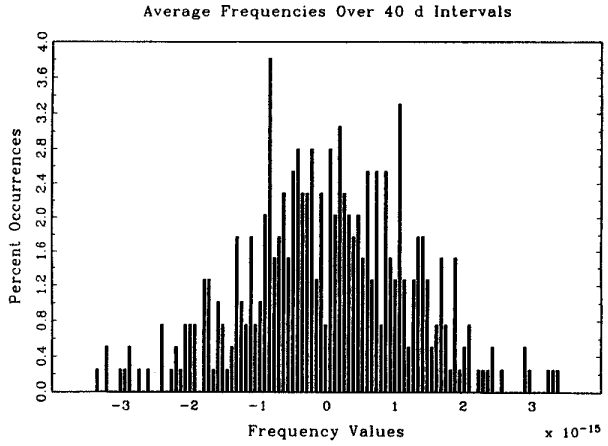


Figure 7 Distribution of frequency uncertainty values.

If one assumes that the time-transfer noises of GPS common-view and TWSTFT are equal, then $\sigma_{tt}(T,\tau)$ in Fig. 6 can be divided by $\sqrt{2}$ and it will take T = 34 days to achieve $1x10^{-15}$ using either technique alone. Another factor of $\sqrt{2}$ is gained if both GPS common-view and TWSTFT data (assumed to be independent) are available for determining the frequency difference of the two LO's and the two are averaged. This reduces the comparison time to 24 days to achieve a frequency uncertainty of $1x10^{-15}$ in the time transfer. In fact, by averaging the data from two independent time-transfer systems the frequency uncertainty is one half the combined noise ($\sigma_{tt}(T,\tau)$ in Fig. 6) no matter what the relative noise levels of either time-transfer system are. This approach is not optimum if one of the transfer systems is much quieter than the other, but it is the best that can be achieved if the individual noise levels are not known. Another advantage of using two time-transfer techniques during a fountain comparison is the ability to more easily identify unusual events in the time-transfer processes.

$\sigma_y(\tau)$ and Mod $\sigma_y(\tau)$ have also been calculated from the data set used for Fig. 6. $\sigma_y(\tau)$ is about 20% larger then $\sigma_{tt}(T,\tau)$ at $\tau$ = 40 days, while Mod $\sigma_y(\tau)$ is 30% smaller. It is not surprising that the Allan variances are in reasonably good agreement with $\sigma_{tt}(T,\tau)$ since the noise characteristic of the data in Fig. 6 is a fairly well behaved flicker of phase. The Allan variances work well as a measure of frequency uncertainty if the noise levels are stable over time, the instabilities fall into the category of one of the standard noise processes, and enough time has been available to adequately characterize the slow processes. However, instabilities in complex systems such as a time-transfer system may not be this well behaved. The Allan variances can underestimate the frequency uncertainty in situations where slow systematic processes, such as seasonal variations, are present if: (1) insufficient time has been available to adequately characterize them, and/or (2) they are not stationary.

It is important to note that $\sigma_{tt}(T,\tau)$ can be used to characterize frequency uncertainty only on a time series where clock noise and the clock offset have been eliminated, such as in Fig. 3 where two transfer techniques are compared. It is of no use in a situation where a clock frequency offset dominates the time-transfer noise characteristics.

An evaluation interval of 24 to 40 days to compare two cesium-fountain primary standards is an uncomfortably long period of time. Therefore, it is very desirable to have more stable time-transfer techniques. Common-view GPS can be improved by using measured ionospheric corrections and precise ephemerides [2]. Also an "all in view" approach using multichannel receivers can be helpful [3]. Use of the P-code would yield even

more impressive results but this would require classified receivers or using GLONASS [2]. However, the most promising GPS technique is to use the carrier phase for time transfer. Preliminary results have been very encouraging and this technique should reduce the time-transfer noise by an order of magnitude [4]. This would reduce the comparison time to about 4 days or less at the $1x10^{-15}$ level. Improvements in TWSTFT may also give substantially reduced instabilities [5]. However, none of these techniques are fully proven or operational yet. Therefore, it is likely that the first fountain comparisons will be made with common-view GPS and/or TWSTFT. If possible, ionospheric and precise orbit corrections should be made to the GPS data, but a long comparison time will still be required. All of the above techniques can be degraded by instabilities in the ground-based equipment, which in many cases are caused by environmental sensitivities. Thus the use of any particular technique doesn't guarantee good performance.

## Fountain Dead Time

Because of laser-lock problems operating a fountain continuously for tens of days can be a difficult task and may not be possible in the first generation of fountains. Therefore it is important to understand the impact of fountain dead time on the uncertainty of a frequency comparison. In particularly we are interested in distributed dead time. Figure 8, adapted from Barnes and Allan [6], illustrates how distributed dead-time parameters are defined. Here the vertical axis is fractional frequency, y(t), rather than time difference. T represents the total measurement interval, $\tau_0$ is the duration of an individual 'live' time measurement, $T_0-\tau_0$ is the dead time between

$T = MT_0$ = measurement interval
M = number of live measurements in T
$\tau = M\tau_0$ = total live time $T > \tau$

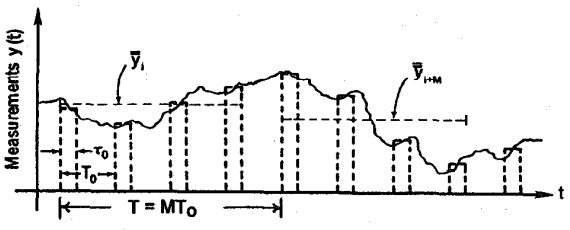


Figure 8 Definition of dead-time parameters.

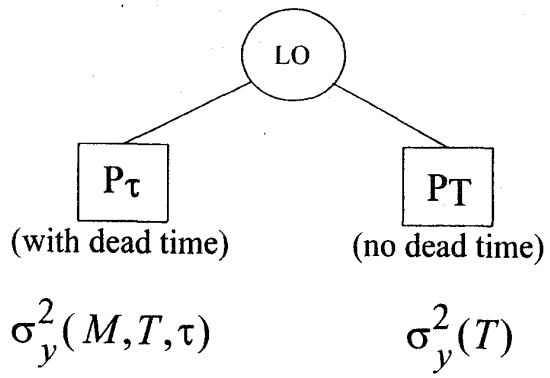


Figure 9 Frequency uncertainty due to dead time.

live time measurements, and M is the number of live time measurements in the interval T. The total live time is $\tau = M\tau_0$, and the total dead time is $T-M\tau_0$. We will only consider the case were $T \geq \tau$. For the example in Fig. 8 there are 4 measurements of duration $\tau_0$ distributed evenly over T. The four measurements in Fig. 8 are not symmetric about the center of T, whereas in a fountain comparison every effort should be made to make them as symmetric as possible since this minimizes the error caused by frequency drift.

Figure 9 illustrates how dead time contributes to the uncertainty of a frequency measurement. Consider a local oscillator, LO, being measured by two identical, ideal frequency standards, $P_\tau$ and $P_T$. The measurement made with no dead time by $P_T$ will be considered the 'truth', while a simultaneous measurement by $P_\tau$ with dead time is an estimate of the truth. The measurement of $\bar{y}_d(t)$ with dead time is therefore an estimate of $\bar{y}(t)$ measured without dead time. What we want to know is the uncertainty, $\sigma_d$, of the estimate. Douglas et al [7] have calculated $\sigma_d$ for lumped dead time. From [6] and [7] it can be shown that the measurement uncertainty, $\sigma_d(M,T,\tau)$, is related to the Allan variances with and without dead time as shown in Eq. 2,

$$\sigma_d^2(M,T,\tau) \approx \sigma_y^2(M,T,\tau) - \sigma_y^2(T), \quad (2)$$

where $\sigma_y(M,T,\tau)$ is the Allan deviation with dead time and $\sigma_y(T)$ is the Allan deviation over interval T without dead time. M = 1 for lumped dead time. From [6] we find that $\sigma_y(M,T,\tau)$ is always larger than $\sigma_y(T)$ for white, flicker, and random-walk frequency noise (with or without distributed dead time) for the case where $T > \tau$ . For $T = \tau$, we find as expected that $\sigma_y(M,T,\tau) = \sigma_y(T)$. The

relation in Eq. 2 is exact for white frequency noise. For flicker and random-walk frequency noise it is only approximate, with errors in calculating $\sigma_d(M,T,\tau)$ no larger than +/- 50% for lumped dead times ranging from 50% to 97%.

It is clear from [6] that distributed dead time gives a better measure of the true Allan deviation for flicker and random-walk noise than does lumped dead time with the same $\tau$. For white frequency noise it makes no difference whether the dead time is lumped or not. Since distributed dead time gives a better estimate of the true Allan deviation for flicker and random-walk noise every effort should be made to spread the dead time evenly throughout the interval T, as this gives a smaller value for $\sigma_d(M,T,\tau)$. Unfortunately exact solutions are not available for $\sigma_d(M,T,\tau)$ with distributed dead time (except for white frequency noise) so values of $\sigma_y(M,T,\tau)$ from [6] along with Eq. 2 have to be used.

From [6], [7] and Eq. 2 we obtain the expressions below. Equation 3 gives the Allan deviation with dead time for white frequency noise and Eq. 4 gives the measurement uncertainty.

White Frequency

$$\sigma_y(T,\tau) = \sqrt{\frac{T}{\tau}}\sigma_y(T) \qquad (3)$$

$$\sigma_d(T,\tau) = \sqrt{(\frac{T}{\tau}-1)}\sigma_y(T) \qquad (4)$$

Equations 5 and 6 give respectively the Allan deviation and measurement uncertainty with distributed dead time for flicker frequency noise.

Flicker Frequency

$$\sigma_y(M,T,\tau) = \sqrt{B_2B_3}\sigma_y(T) \qquad (5)$$

$$\sigma_d(M,T,\tau) \approx \sqrt{(B_2B_3-1)}\sigma_y(T) \qquad (6)$$

$B_2$ and $B_3$ are bias coefficients tabulated in [6] which are functions of M, T, $\tau$, and the noise type. Equations 7 and 8 give respectively the Allan deviation and measurement uncertainty with distributed dead time for random-walk frequency noise.

Random-walk Frequency

$$\sigma_y(M,T,\tau) = \sqrt{\frac{\tau}{T}B_2B_3}\sigma_y(T) \qquad (7)$$

$$\sigma_d(M,T,\tau) \approx \sqrt{(\frac{\tau}{T}B_2B_3-1)}\sigma_y(T) \qquad (8)$$

Note that $B_2$ and $B_3$ for random-walk noise do not have the same values as for flicker noise and are also dependent on M, T, $\tau$. It would be very desirable to have exact expressions for $\sigma_d(M,T,\tau)$ for distributed dead time with flicker and random-walk noise but that is beyond the scope of this paper.

Consider now an example of distributed dead time using a cavity-tuned hydrogen maser as the LO. The noise characteristics without dead time of a better than average (but not the best) maser at NIST are shown below for the three relevant noise types. $\tau$ is in units of 1 day. It is difficult to accurately characterize the random-walk noise level because of the large frequency drift in hydrogen masers, but the number used is reasonably conservative.

White Frequency

$$\sigma_y(\tau) = (6.8\text{x}10^{-16})\tau^{-1/2}$$

Flicker Frequency

$$\sigma_y(\tau) = (3.0\text{x}10^{-16})$$

Random-walk Frequency

$$\sigma_y(\tau) = (4.4\text{x}10^{-17})\tau^{1/2}$$

For dead-time parameters we will use T = 40 days, M= 8, and $M\tau_0 = \tau = 5$ days. This gives values of $\sigma_d(M,T,\tau)$ for each noise type as shown below. For flicker and random-walk noise we have assumed maximum errors comparable to those calculated for the lumped dead-time estimates when using Eq. 2.

White Frequency

$$\sigma_d(8,40,5) = 2.65(1.1\text{x}10^{-16}) = 2.9\text{x}10^{-16}$$

Flicker Frequency

$$\sigma_d(8,40,5) < 0.5(3.0\text{x}10^{-16}) = 1.5\text{x}10^{-16}$$

Random-walk Frequency

$$\sigma_d(8,40,5) < 0.12(2.8\text{x}10^{-16}) = 3.4\text{x}10^{-17}$$

The example above shows that even with 35 out of 40 days of dead time (87%) a cavity-tuned hydrogen maser provides a sufficiently good local oscillator that the total measurement uncertainty (root sum square of the three values above) is less than $3.3\text{x}10^{-16}$. Even if the dead time is lumped (for which there are exact expression) the total measurement uncertainty is only $5.1\text{x}10^{-16}$. It is important to note that care should be taken to make the live time measurements evenly spaced and as symmetric about the center of T as possible to ensure that frequency drift does not excessively bias the measured frequency.

As T gets smaller the fraction of dead time that can be tolerated also gets smaller. This is because white frequency noise is one of the major sources of measurement uncertainty. For example, if T = 5 days, a dead time of only 2.5 days (50%) will give the same measurement uncertainty for white frequency noise as in the example above. Depending on the details of the dead time, the contributions from flicker and random-walk noise may be the same as or smaller than in the example.

## Summary

The analysis presented here has shown that if common-view GPS and/or TWSTFT are used to compare the frequencies of two primary frequency standards it will take at least 24 and possibly 40 days to reduce the frequency uncertainty introduced by the time-transfer process to the range of $1 \times 10^{-15}$. It is advantageous to use two or more independent time-transfer techniques during a fountain comparison since this reduces the frequency uncertainty, allows unusual events to be more easily identified, and also permits a statistical analysis based on $\sigma_{tt}(T,\tau)$ to be performed during the actual comparison time.

Twenty to forty days is an uncomfortably long period of time and improved time-transfer techniques are clearly necessary if frequency comparisons are to be performed on a regular basis. However, the situation can be made less painful by using a good local oscillator (such as a hydrogen maser) so that substantial fountain dead time can be present without significantly degrading the uncertainty of the frequency comparison. Again it is important to monitor the performance of the local oscillator during the comparison process to make sure that nothing unusual happens. This can be accomplished with at least one other oscillator of comparable quality, though two or more would be preferred.

## Acknowledgments

We thank the U. S. Naval Observatory for use of their common-view GPS data and PTB for both their GPS and TWSTFT data.

## References

[1] C. Hackman and T.E. Parker, "Noise Analysis of Unevenly Spaced Time Series Data," *Metrologia*, vol. 33, no. 5, pp. 457-466, 1996.

[2] G. Petit and C. Thomas, "GPS Frequency Transfer Using Carrier Phase Measurements," in *Proc. 1996 IEEE International Frequency Control Symposium*, pp. 1151-1158, 1996.

[3] J. Levine, "Time transfer Using Multi-Channel GPS Receivers," in *Proc. 1998 IEEE International Frequency Control Symposium*, (in this Proceedings), 1998.

[4] K. Larson and J. Levine, "Time transfer Using the Phase of the GPS Carrier," in *Proc. 1998 IEEE International Frequency Control Symposium*, (in this Proceedings), 1998.

[5] J.A. DeYoung, F. Vannicola, and A.D McKinley, "A comparison of the highest precision commonly available time-transfer methods: TWSTT and GPS CV," in *Proc. 28th Annual Precise Time and Time Interval (PTTI) Applications and Planning Meeting*, pp. 349-354, 1996.

[6] J.A. Barnes and D.W. Allan, "Variances Based on Data with Dead Time Between the Measurements," *NIST Technical Note 1337*, pp. 296-335, 1990.

[7] R.J. Douglas and J.S. Boulanger, "Standard Uncertainty for Average Frequency Traceability," in *Proc. 11th European Frequency and Time Forum*, pp. 345-349, 1997.